MMEM future experiments, that is not the case in the present-day climate (either in the observation data or the MMEM present experiments). Decadal variability accounts for the calculated linear trend in the present-day climate to a certain degree, mainly because of the short time period of the data. In this work, therefore, we used observation data alone for estimating future interannual variability, and MMEM future results alone for estimating the future linear trend. Correction of the bias in the linear trend between the MMEM present and the observation data might be desirable if the effect of decadal variability could be removed from the calculated linear trend.

If we take the median sea ice concentration of the present-day CGCM experiments, a distribution very similar to the observation data is obtained. Thus, it would be possible to estimate the long-term mean of the locations of future decreases by calculating $fice_{mf} - fice_{\mathrm{mp}}$. However, interannual variability in the location of the decrease is not represented in such a calculation because interannual variability in MMEM is very small as a result of cancellations.

The estimated SST, sea ice concentration, and sea ice thickness have been used as boundary conditions in simulations of an AGCM with a horizontal grid size of 20 km performed by the Earth Simulator. Although the method described in this work would have difficulty estimating values for the very near future, when the phases of the interannual variation would be continuous with the present-day observation data, it is nevertheless one of the most objective methods available by which to estimate sea surface conditions 10 to 100 years from now by using the MMEM results.

Supplementary Information

Monthly SST, sea ice concentration, and sea ice thickness, their changes averaged over the 25 years, and monthly $SST_{\mathrm{mf\_T}}$ and $SST_{\mathrm{obs\_V}}$, are shown in Supplemental Figs. S1–S16.

Acknowledgements

This work was supported by the "Projection of Change in Future Weather Extremes Using Super-High-Resolution Atmospheric Models" project as a part of the KAKUSHIN Program of the Ministry of Education, Culture, Sports, Science and Technology of Japan, and by the Global Environment Research Fund (S-5-2) of the Ministry of the Environment of Japan.

References

Bourke, R.H. and R.P. Garrett, 1987: Sea ice thickness distribution in the Arctic Ocean. *Cold Regions Sci. and Tech.*, **13**, 259-280.

Intergovernmental Panel on Climate Change, 2007: Climate change 2007: The Physical Science Basis—Contribution of the Working Group I to the Fourth Assessment Report of the

Intergovernmental Panel on Climate Change, Cambridge Univ. Press, Cambridge, U. K., 996pp.

Meehl, G., C. Covey, T. Delworth, M. Latif, B. McAvaney, J. Mitchell, R. Stouffer, and K. Taylor, 2007: The WCRP CMIP3 multimodel dataset: A new era in climate change research. *Bull. Am. Meteorol. Soc.*, **88**, 1383–1394.

Rayner, N. A., D. E. Parker, E. B. Horton, C. K. Folland, L. V. Alexander, D. P. Rowell, E. C. Kent, and A. Kaplan, 2003: Global analyses of sea surface temperature, sea ice, and night marine air temperature since the late nineteenth century. *J. Geophys. Res.*, **108(D14)**, 4407, doi:10.1029/2002JD002670.

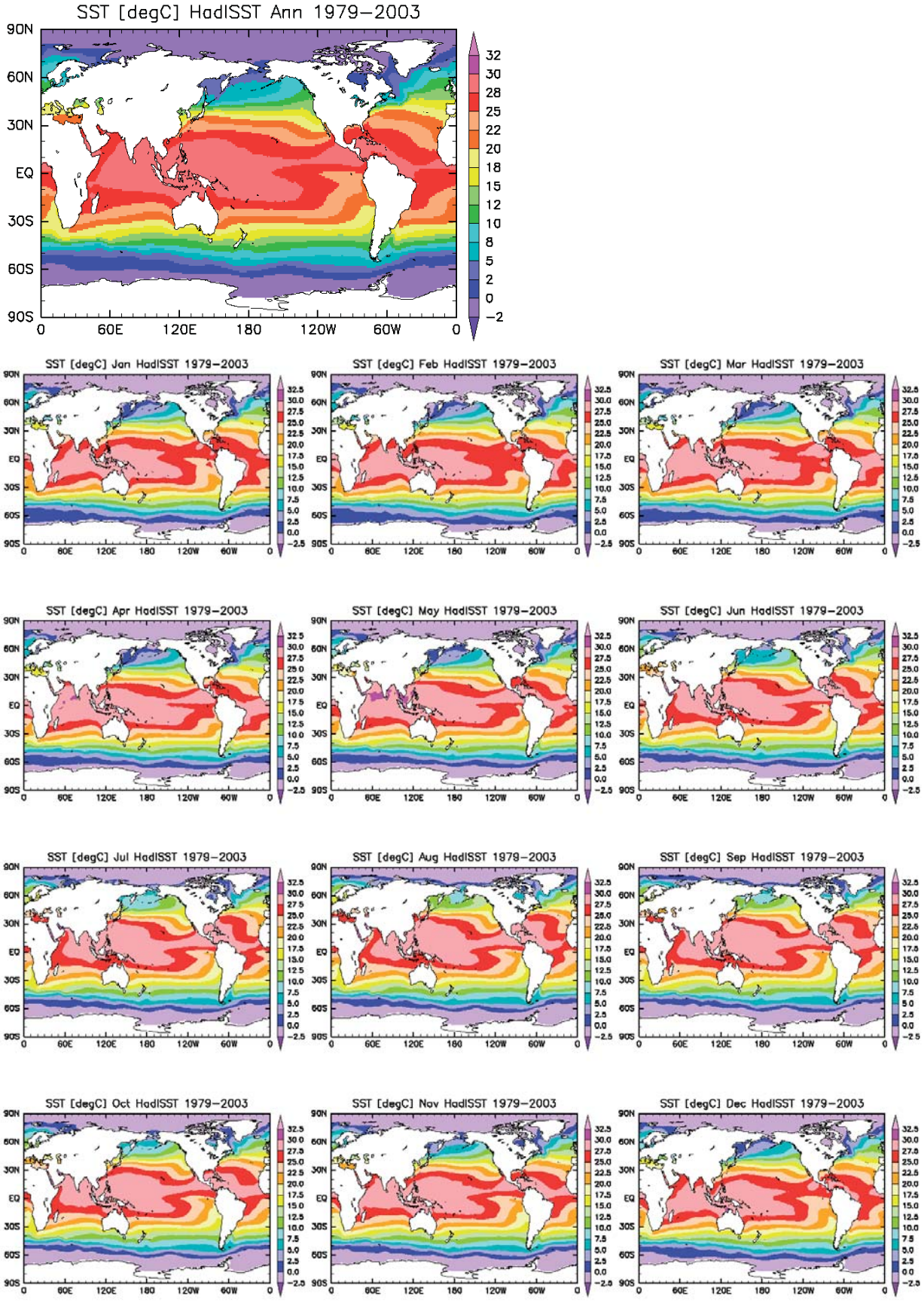

Fig. S1: Observational distributions of annual mean SSTs and monthly SSTs averaged from 1979 to 2003.

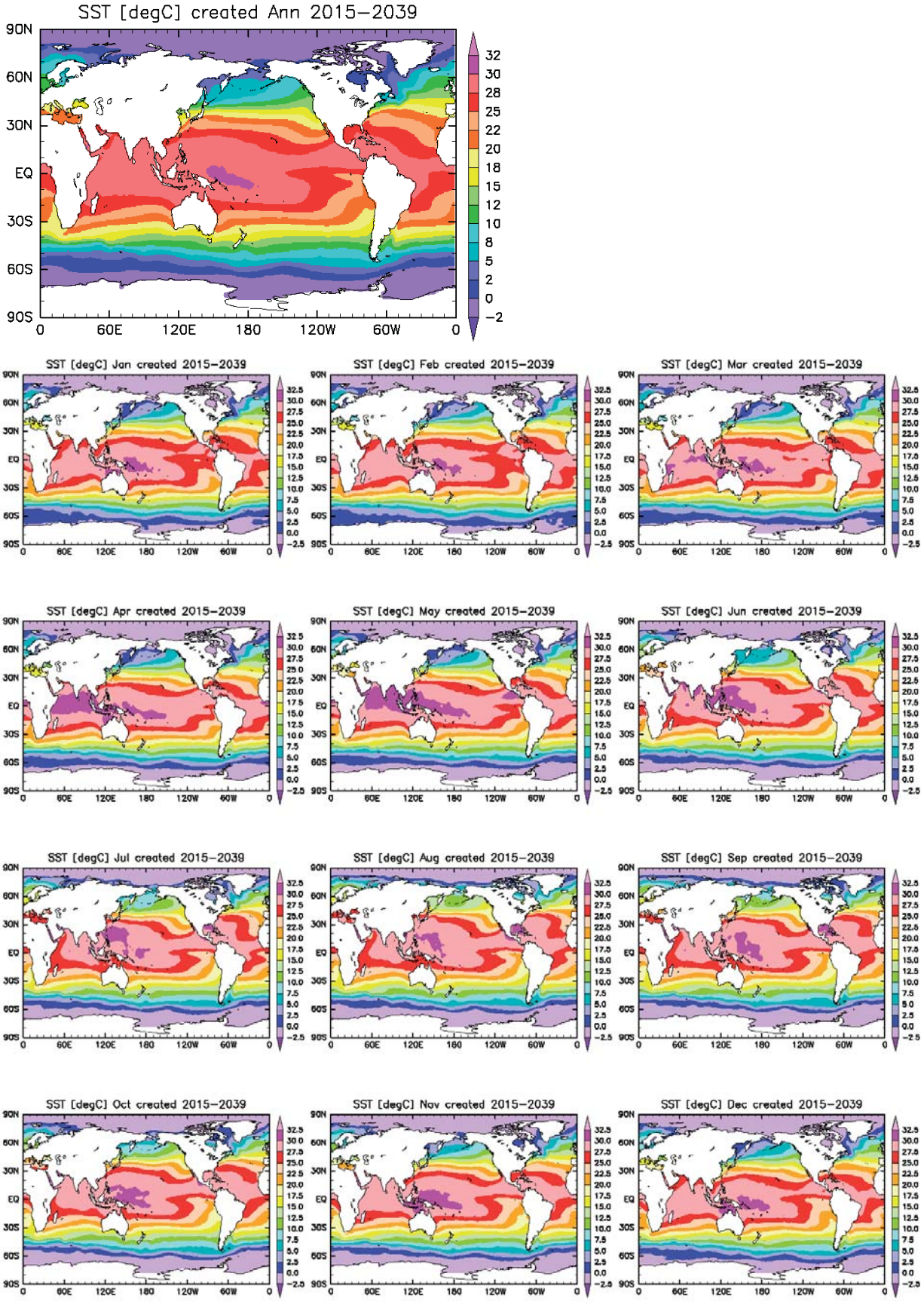

Fig. S2: Estimated near-future distributions of annual mean SSTs and monthly SSTs, averaged from 2015 to 2039.

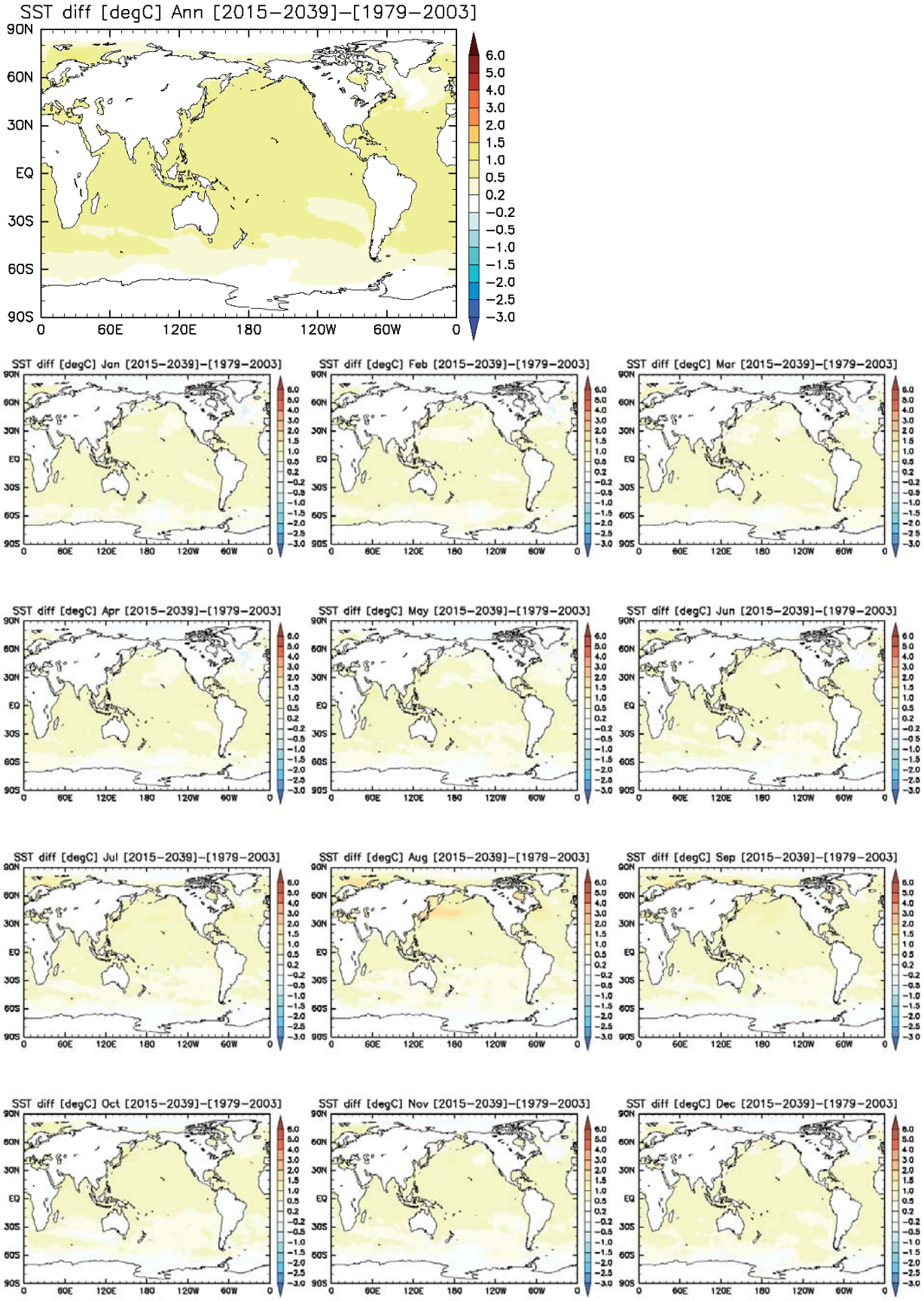

Fig. S3: Differences in the annual mean SSTs and monthly SSTs between the observation data (1979–2003) and the estimated near-future values (2015–2039).

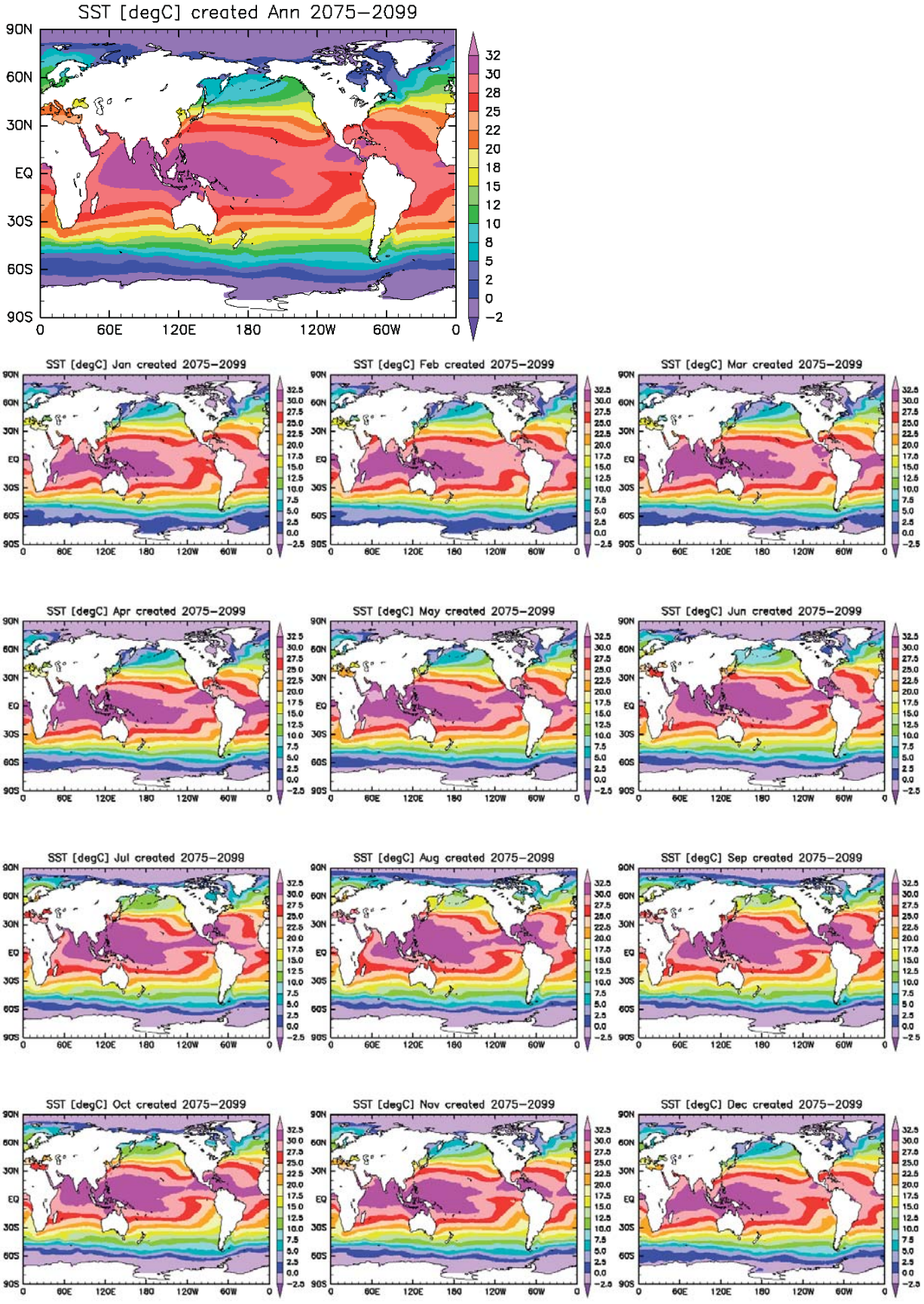

Fig. S4: Estimated future distributions of annual mean SSTs and monthly SSTs averaged from 2075 to 2099.

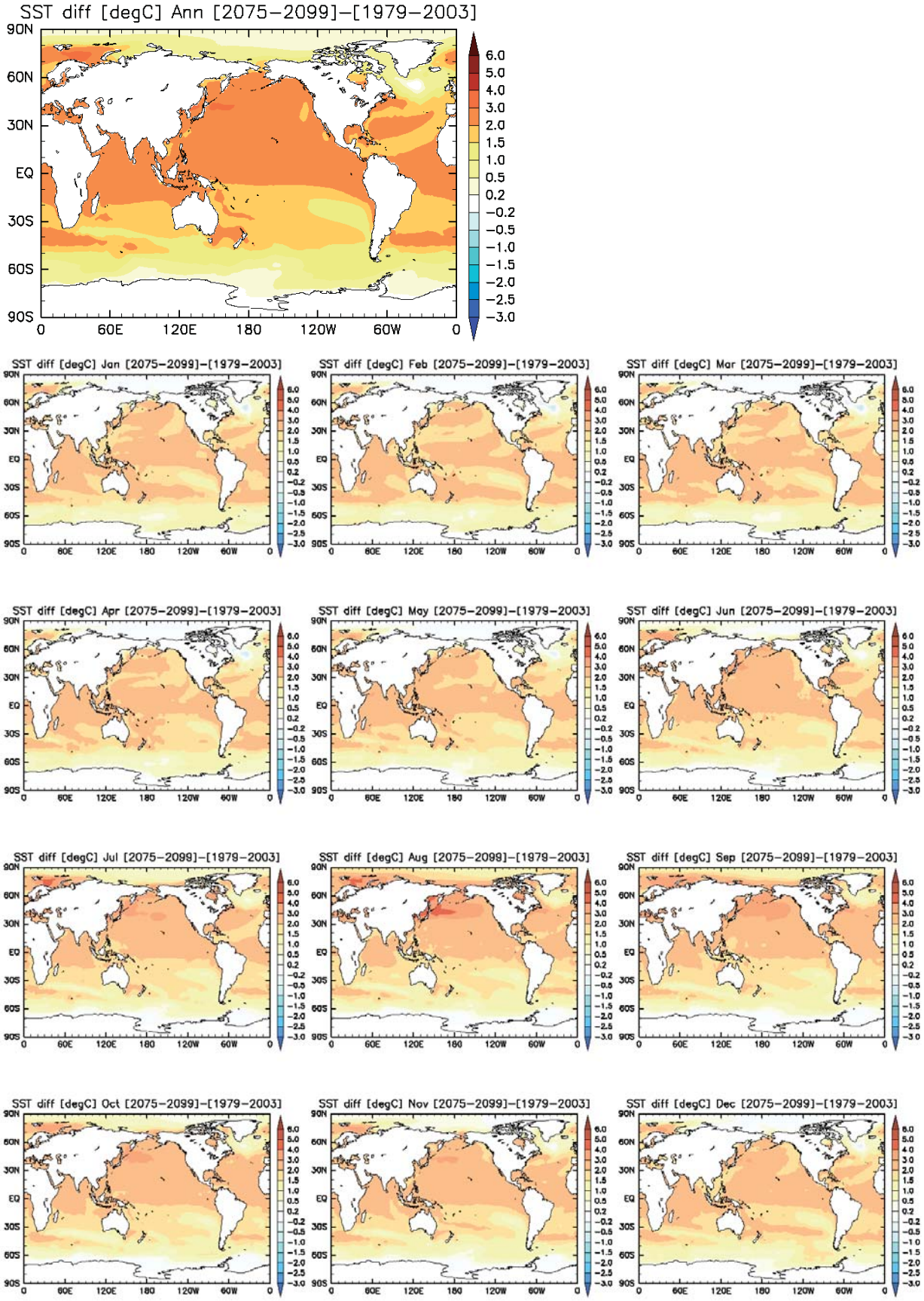

Fig. S5: Differences in the annual mean SSTs and monthly SSTs between the observation data (1979–2003) and the estimated future values (2075–2099).

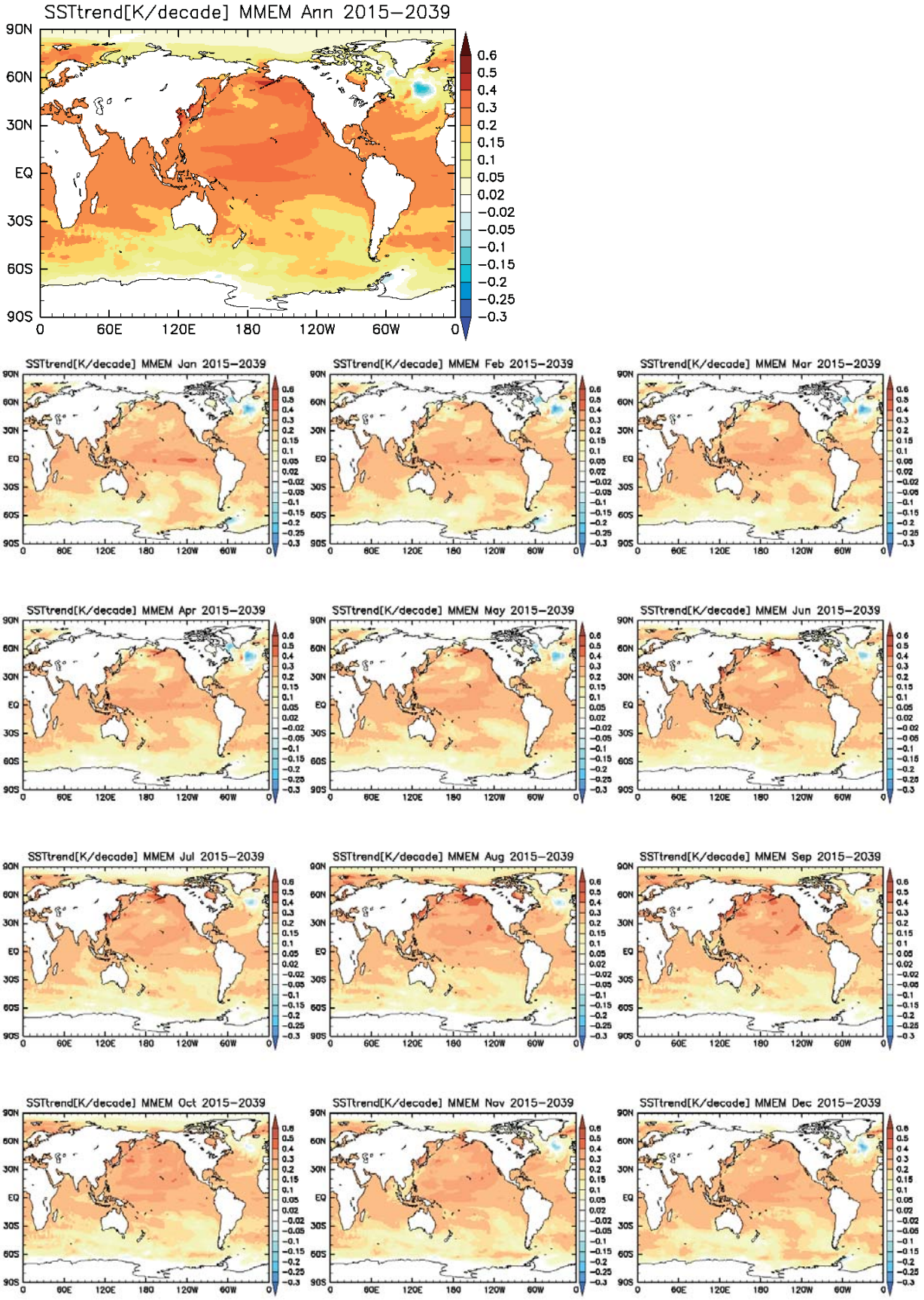

Fig. S6: Linear trends in the multi-model ensemble mean SSTs during 2015 to 2039. Units are K/decade.

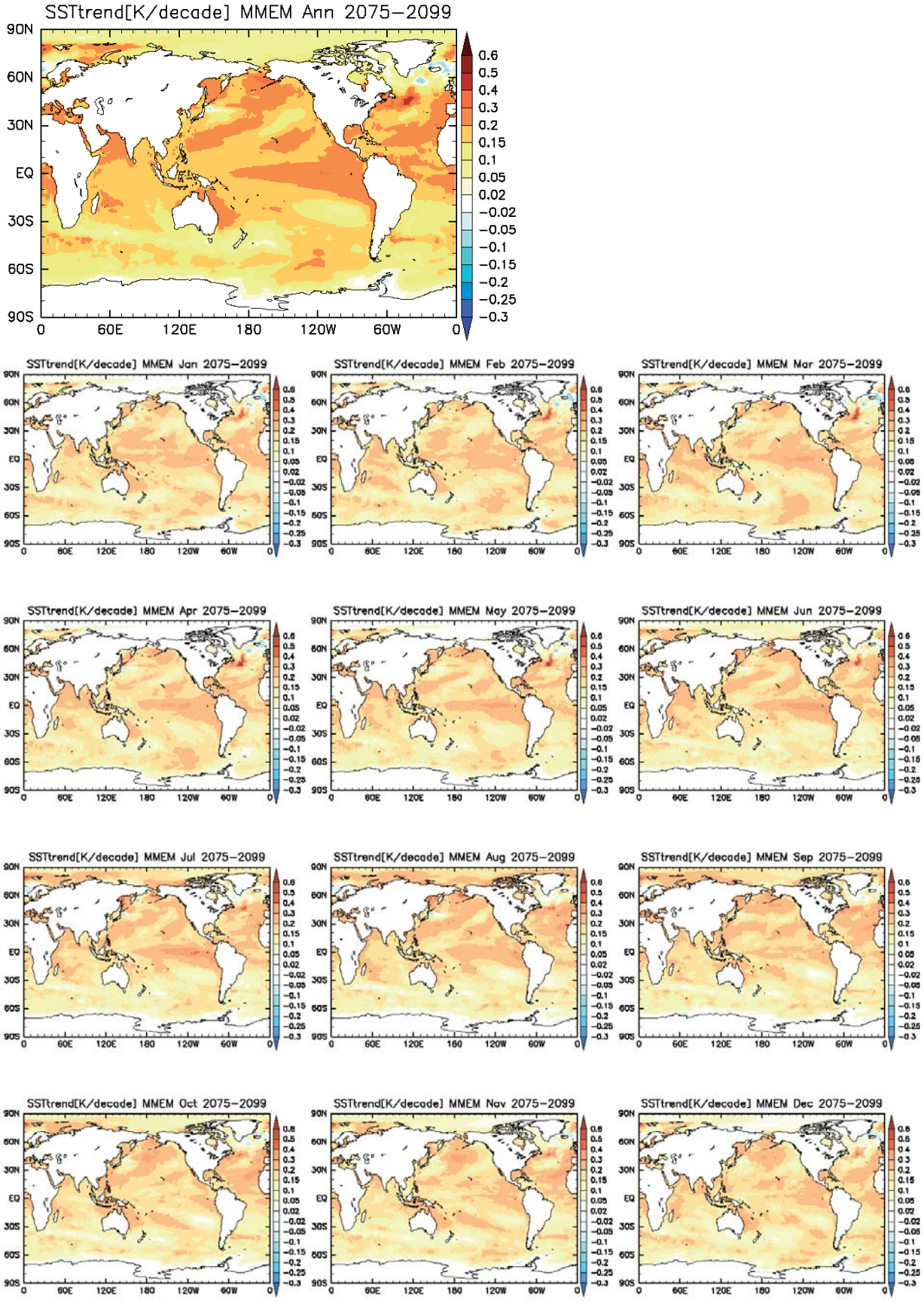

Fig. S7: Linear trends in the multi-model ensemble mean SSTs during 2075 to 2099. Units are K/decade.

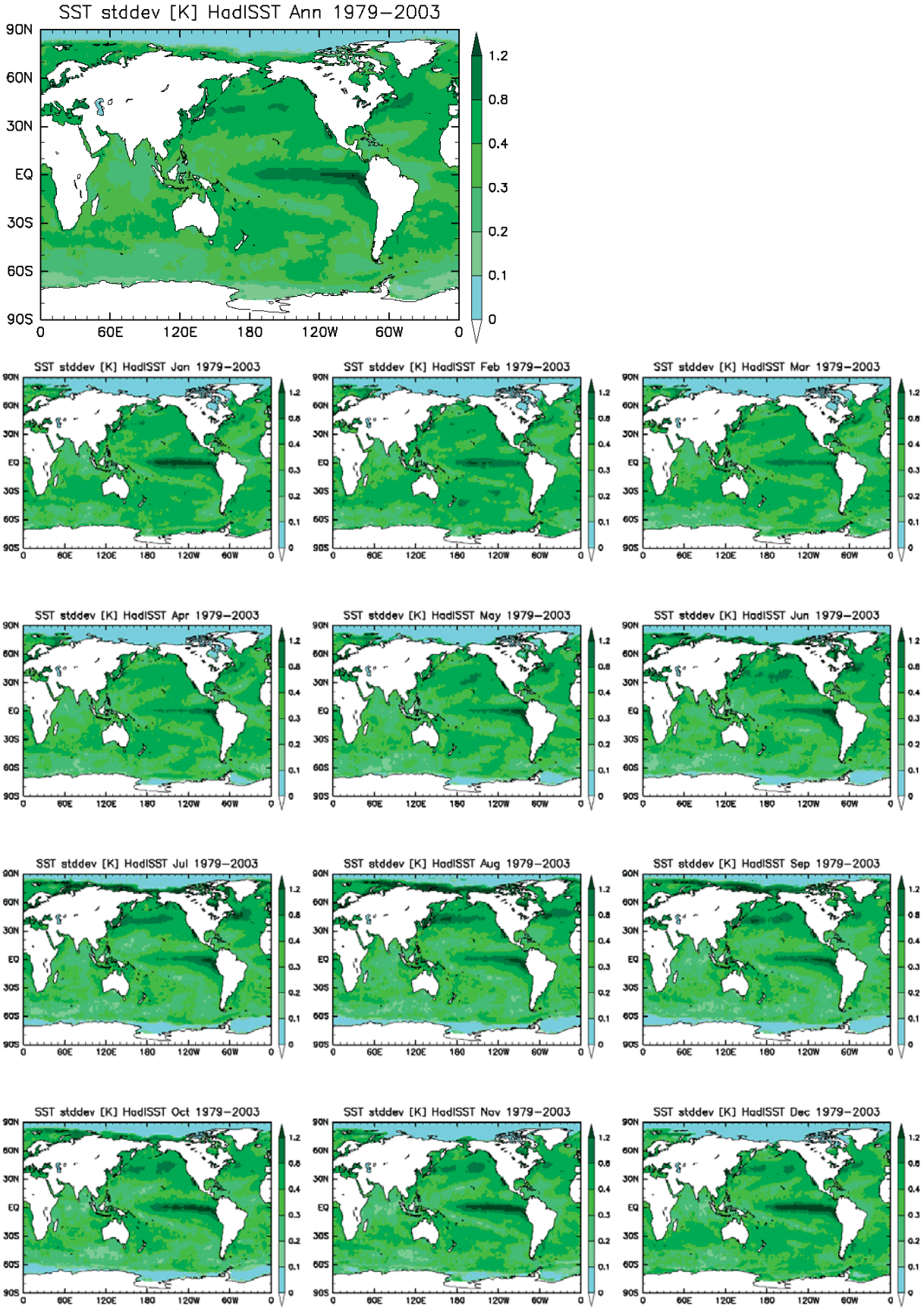

Fig. S8: Standard deviations of the interannual variations in the observed SSTs after removing the linear trend during 1979–2003.

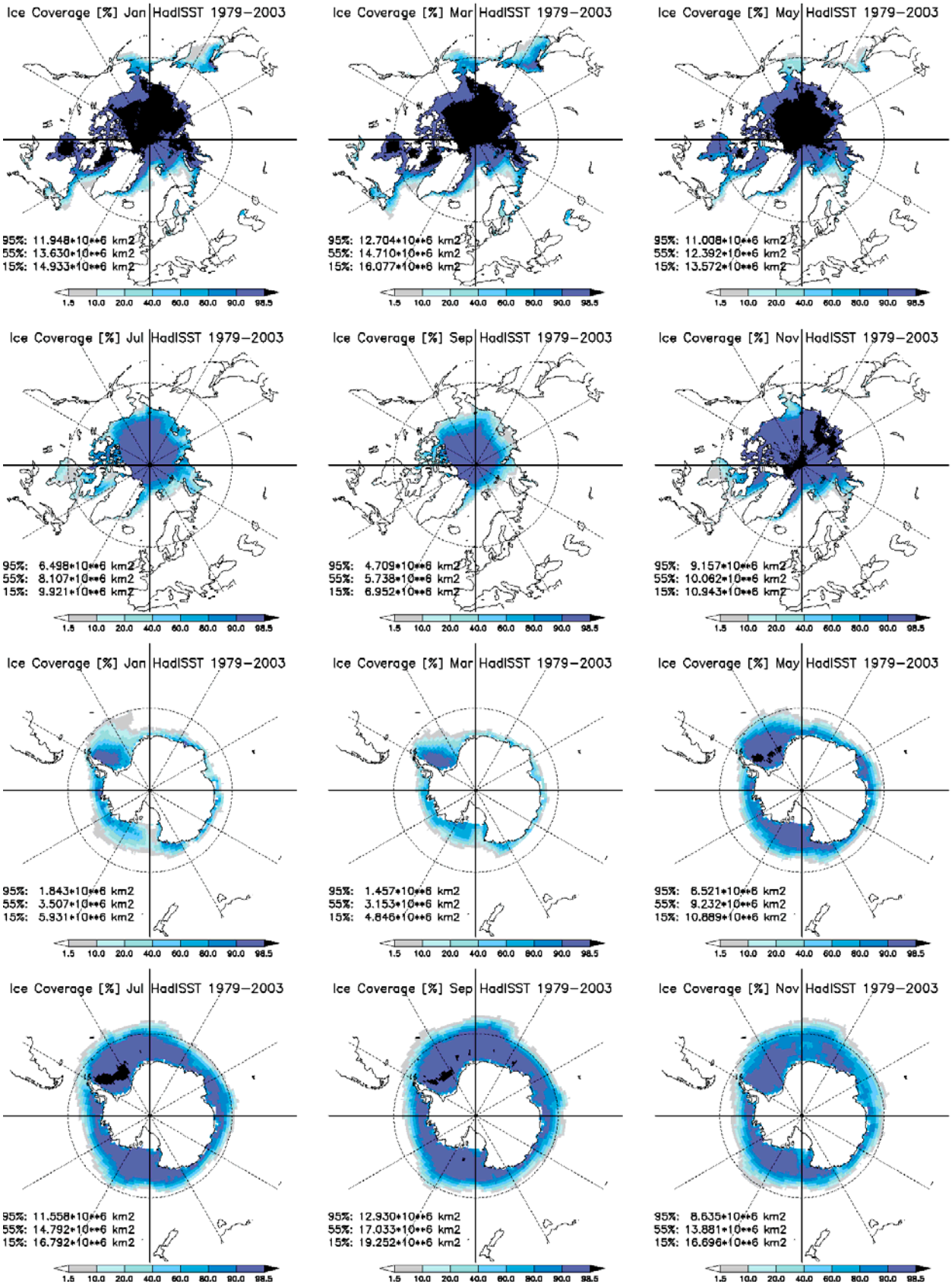

Fig. S9: Observational distributions of monthly sea ice concentrations averaged from 1979 to 2003. The values in the figure denote the sea ice extent for f = 95%, 55%, and 15%.

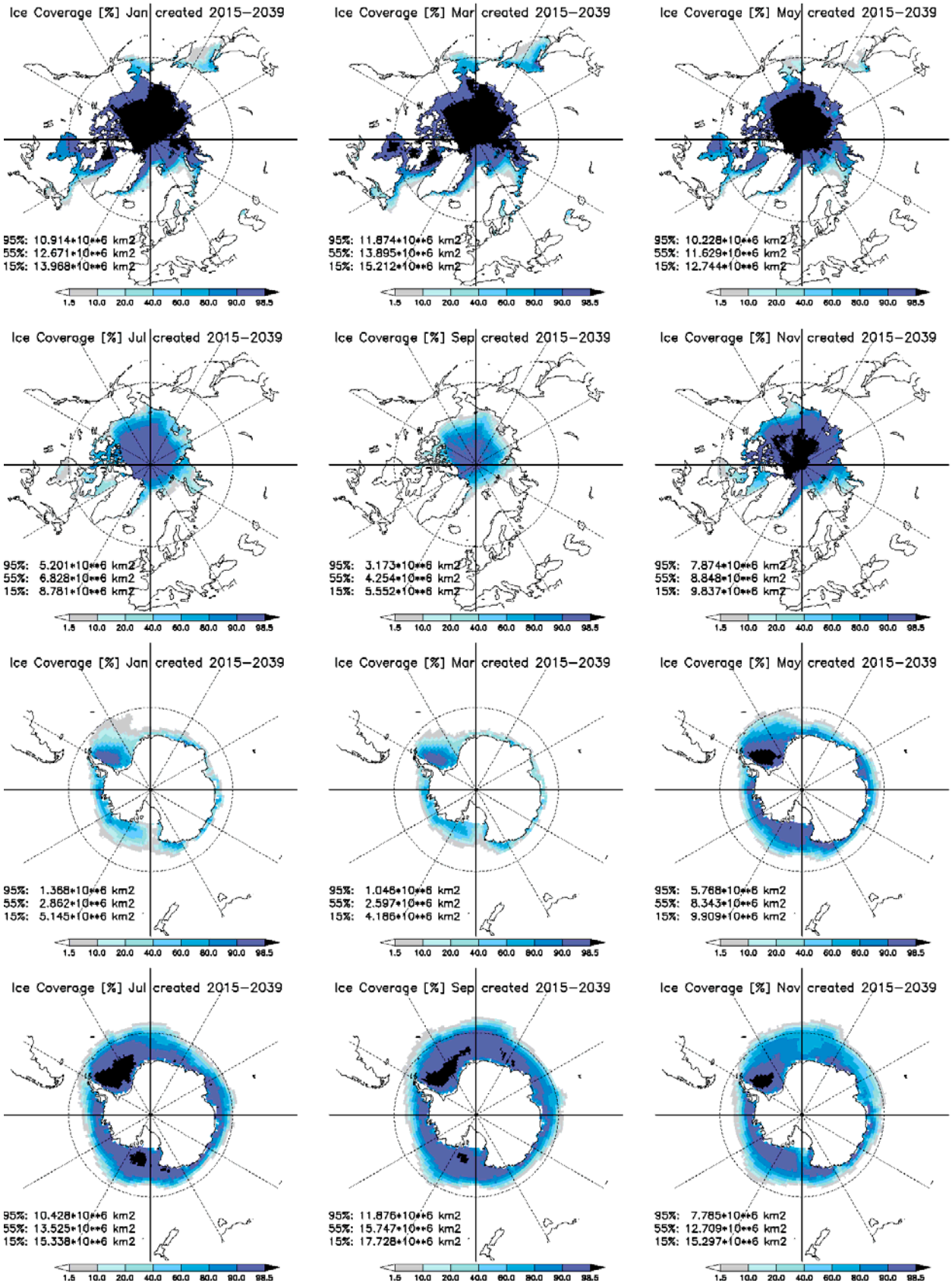

Fig. S10: Estimated near-future distributions of monthly sea ice concentrations averaged from 2015 to 2039. The values in the figure denote the sea ice extent for f = 95%, 55%, and 15%.

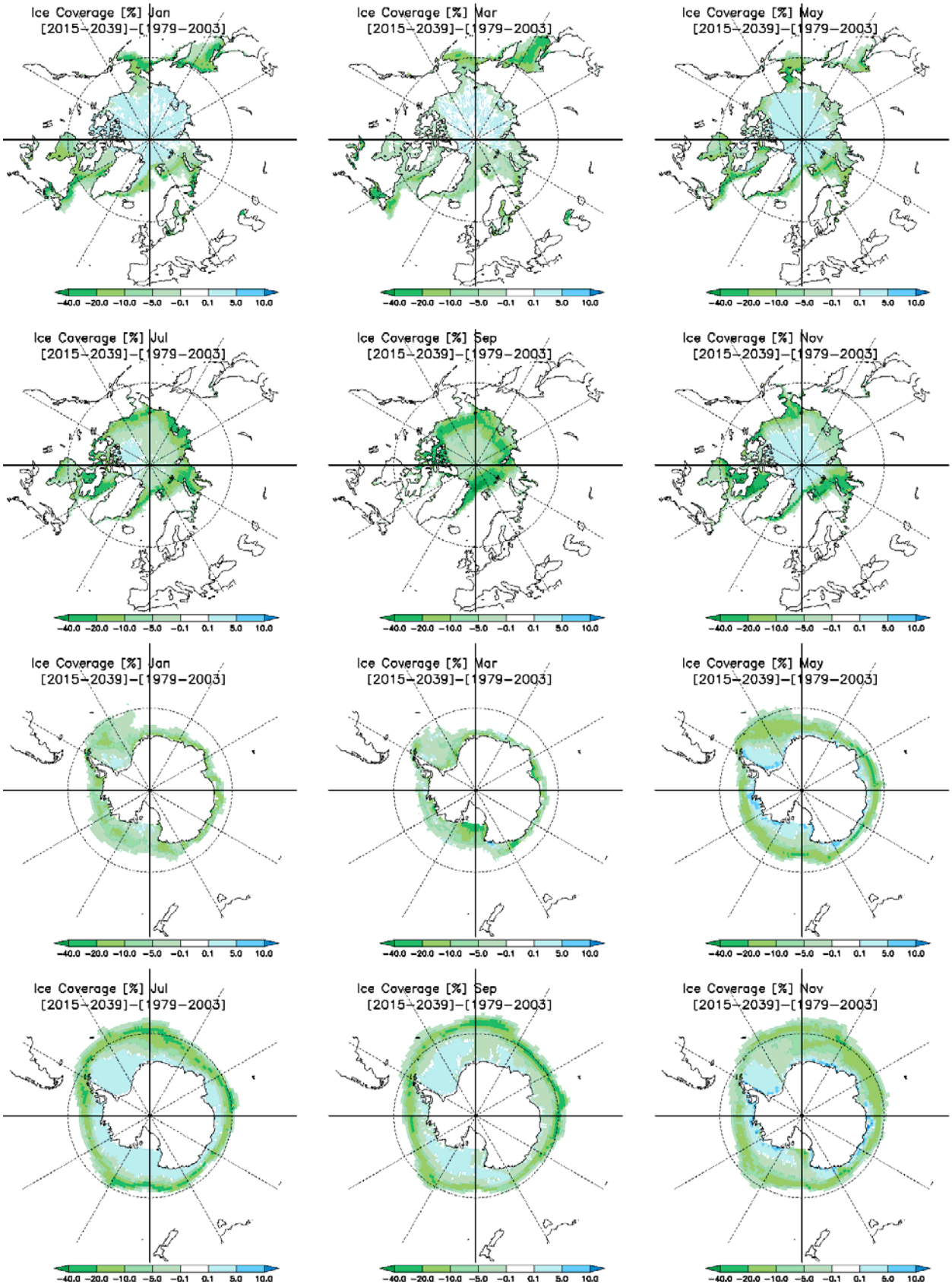

Fig. S11: Differences in monthly sea ice concentrations between the observation data (1979–2003) and the estimated near-future values (2015–2039).

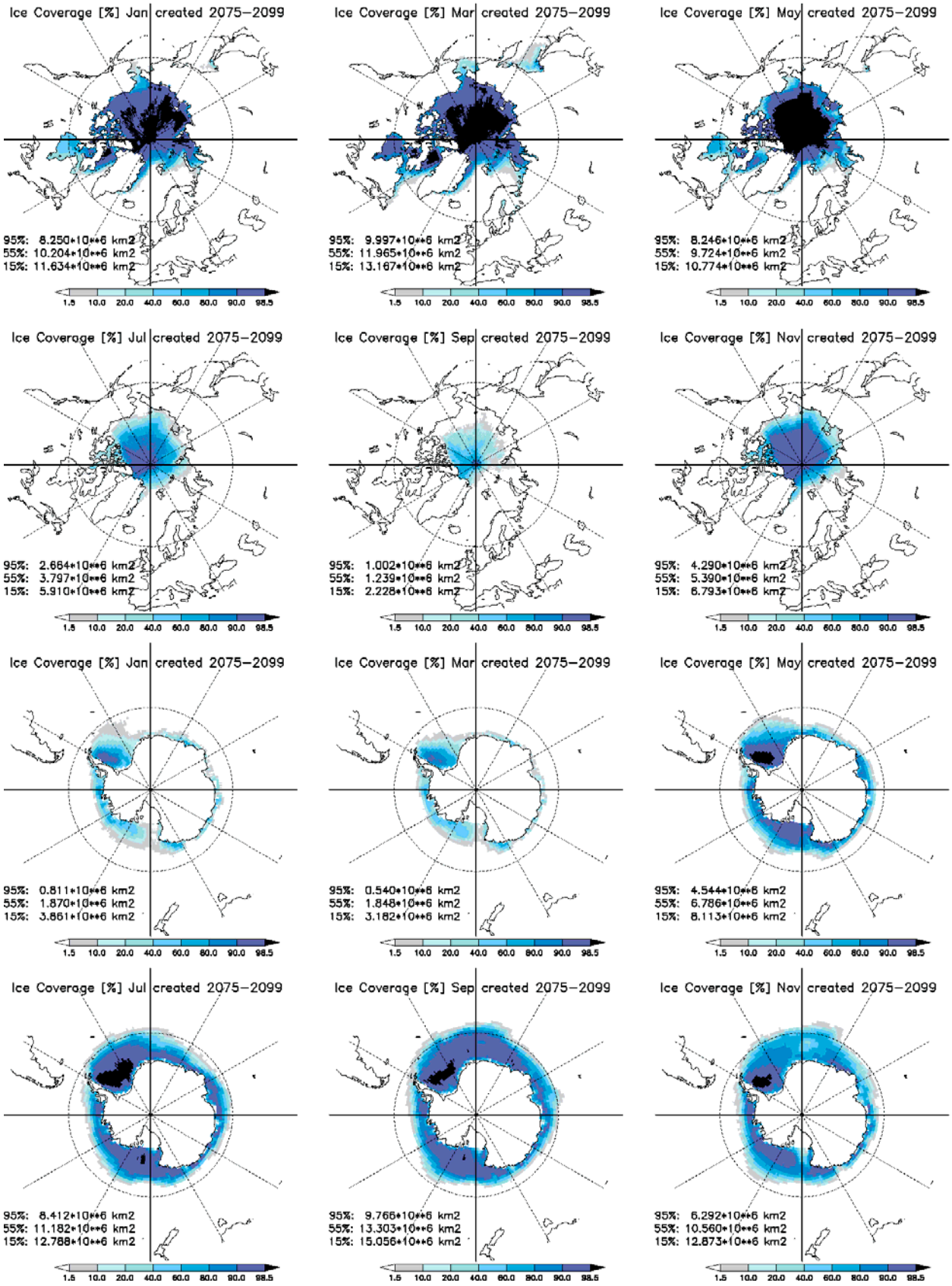

Fig. S12: Estimated future distributions of monthly sea ice concentrations averaged from 2075 to 2099. The values in the figure denote the sea ice extent for f = 95%, 55%, and 15%.

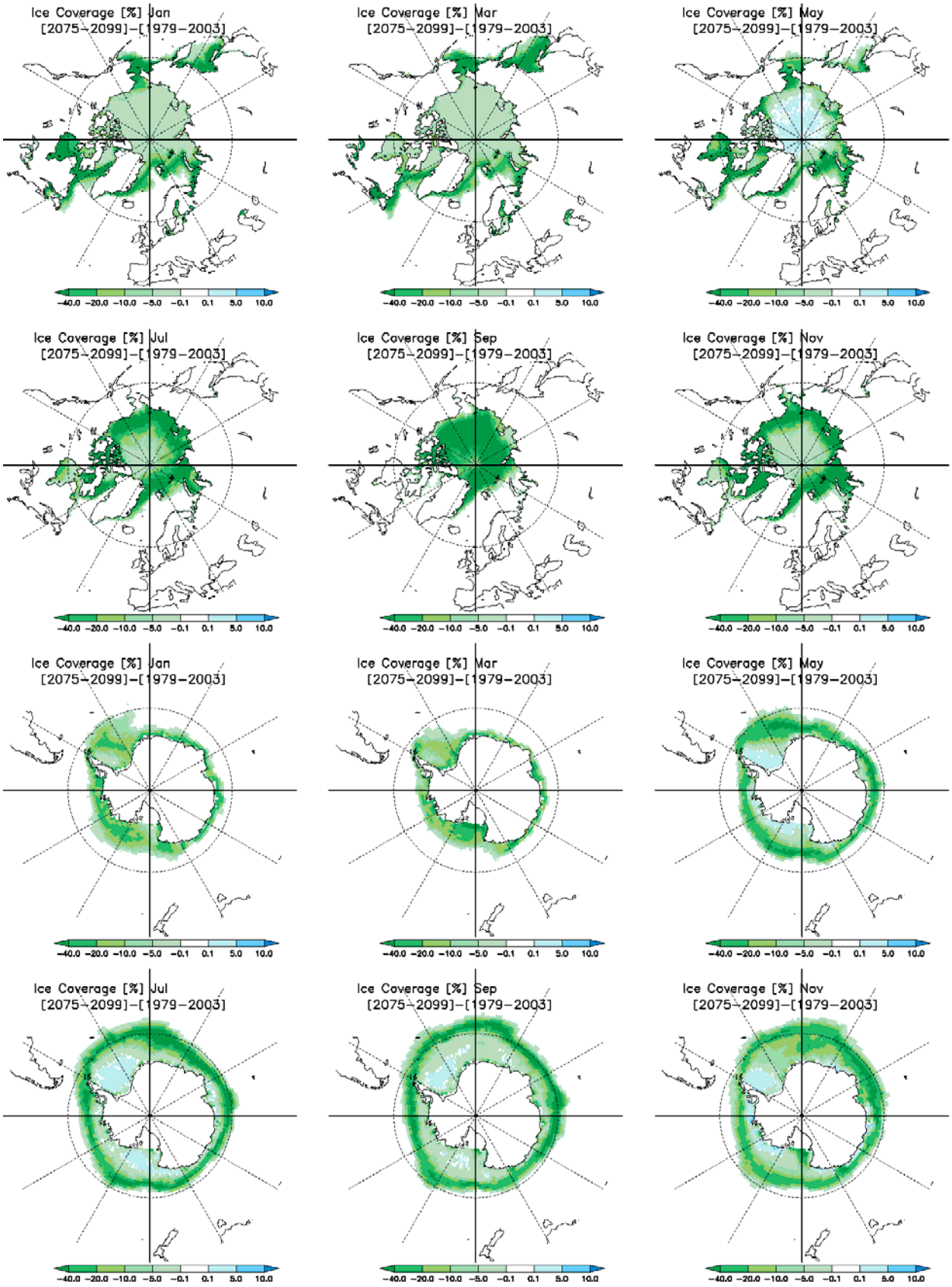

Fig. S13: Differences in monthly sea ice concentrations between the observation data (1979–2003) and the estimated future values (2075–2099).

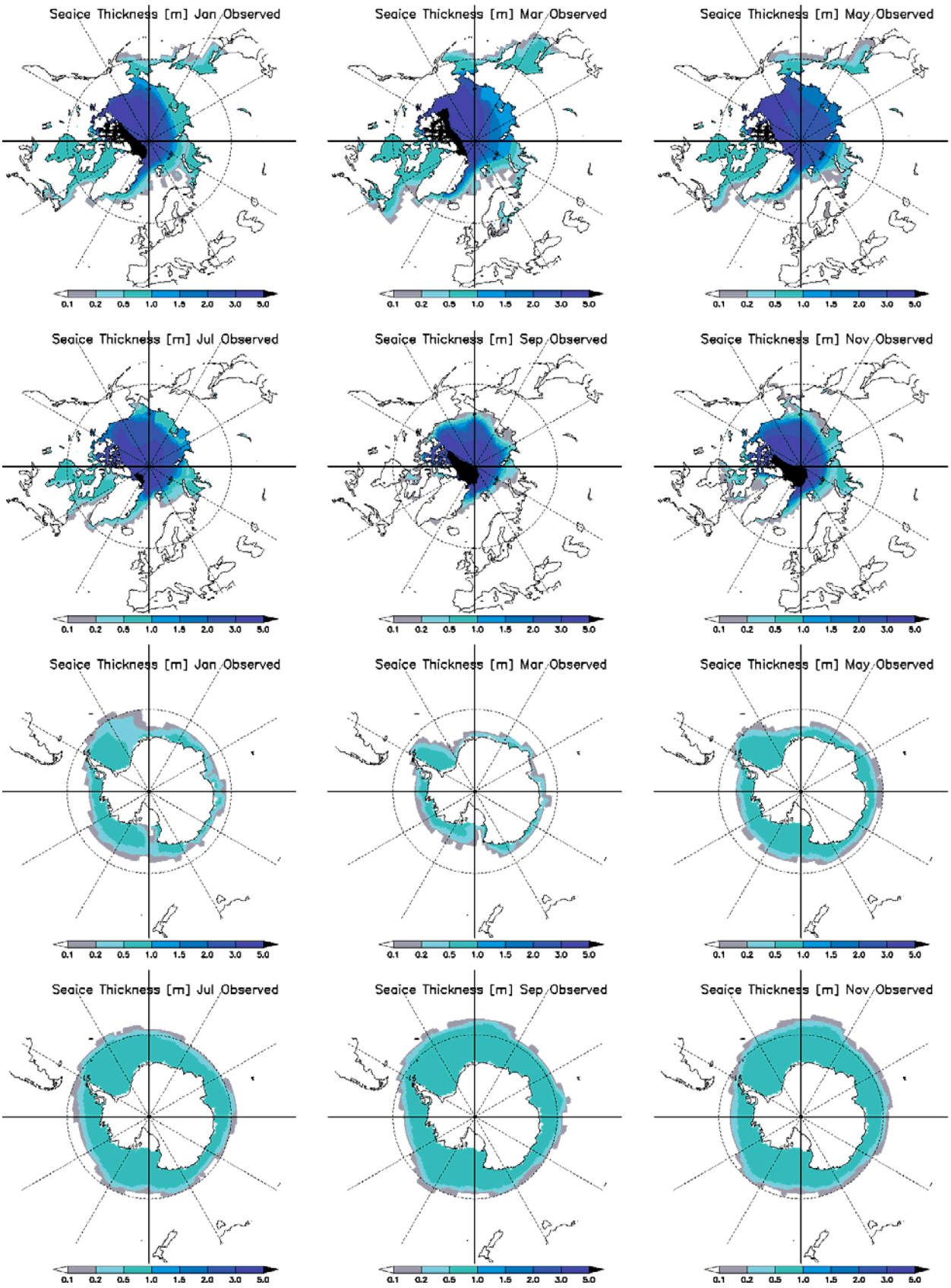

Fig. S14: Observational distributions of monthly sea ice thickness.

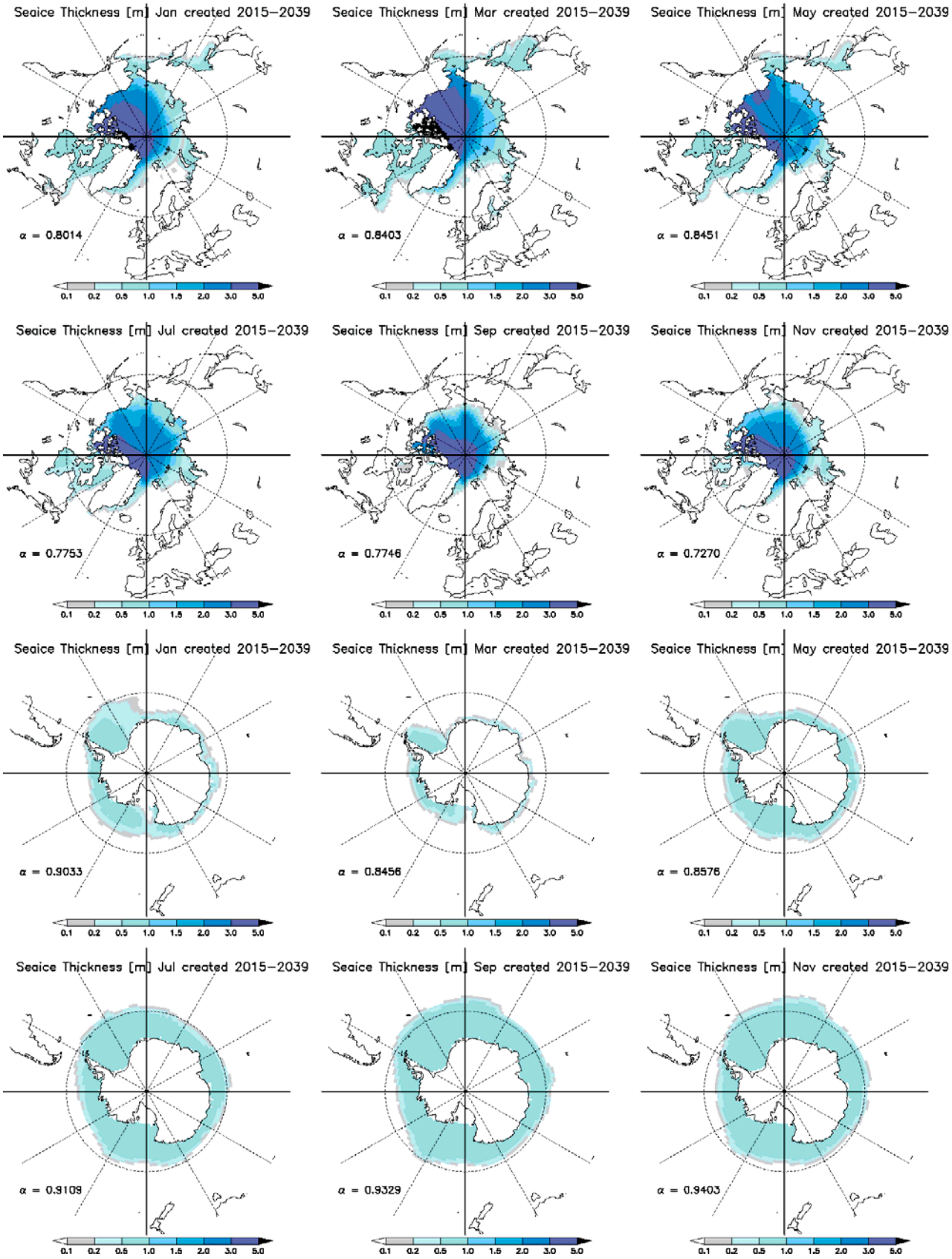

Fig. S15: Estimated near-future (2015–2039) distributions of monthly sea ice thickness. The values of α calculated by Eq. (10) are shown.

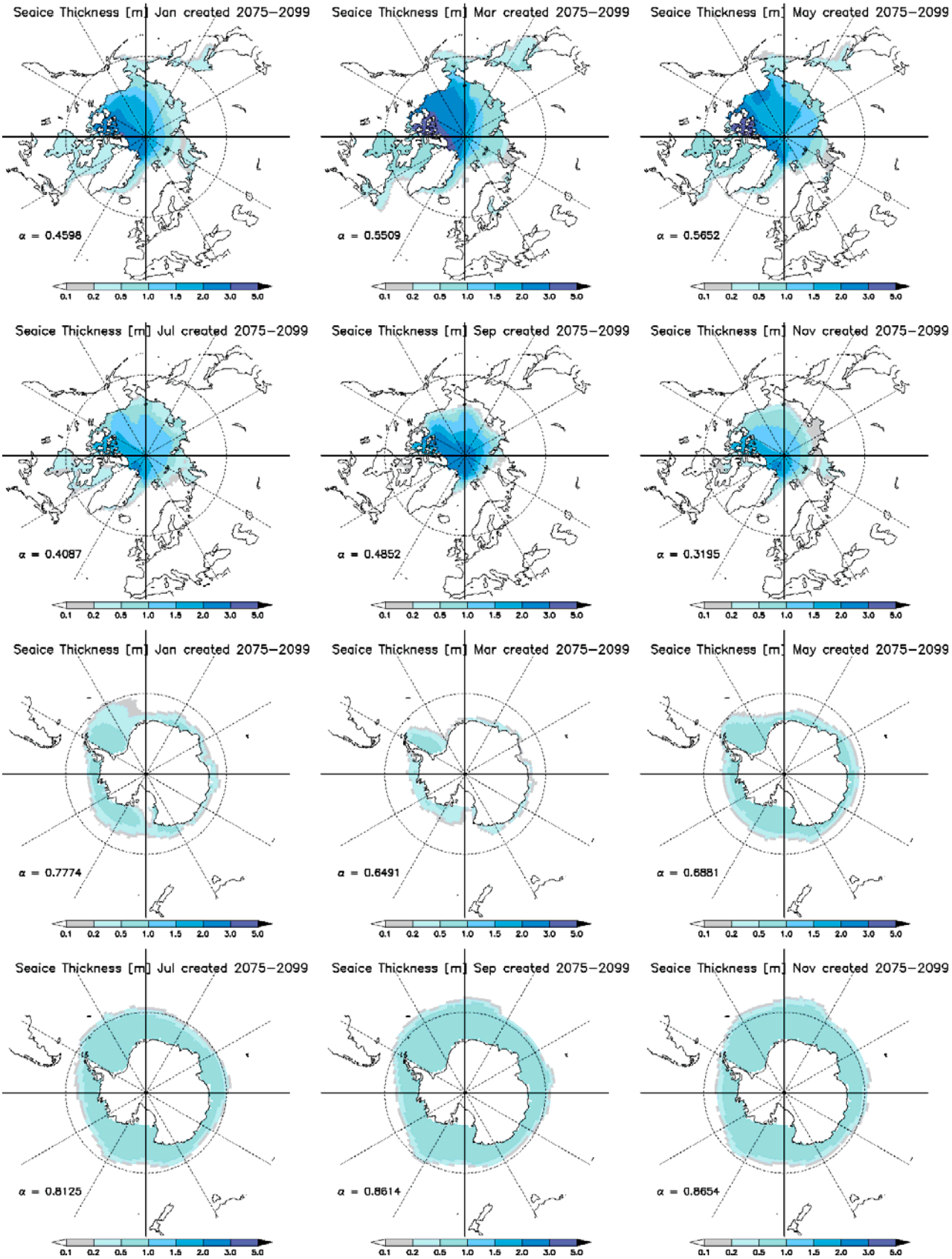

Fig. S16: Estimated future (2075–2099) distributions of monthly sea ice thickness. The values of α calculated by Eq. (10) are shown.